Shahrood University of Technology
Iranian Society of Mining Engineering (IRSME)
Journal of Mining and Environment (JME)
journal homepage: www.jme.shahroodut.ac.ir
THOMSON REUTERS

Geochemical Study of Rare Earth Elements Content in Tabas Coal Ash, Parvadeh Coal Mine

Golnaz Jozanikohan[1*], Mohsen Nosrati Abarghooei[2] and Hasan Sedighi[3]

1- School of Mining Engineering, College of Engineering, University of Tehran, Tehran, Iran
2- Faculty of Mining and Metallurgical Engineering, Yazd University, Yazd, Iran
3- The head of REE project, Iranian Mines & Mining Industries Development & Renovation (Imidro)

Article Info

Received 21 October 2021
Received in Revised form 09 December 2021
Accepted 28 December 2021
Published online 28 December 2021

DOI:10.22044/jme.2022.11319.2114

Keywords

REE Analysis
XRD Method
ICP-MS, REE Distribution
REE Geo-chemistry

Abstract

The most extensive Iranian coal-bearing basin is located in an area of 30000 km2, situated approximately 75 km from the Tabas county, south Khorasan Province, Iran. In this work, the Tabas coal ash is studied and investigated for the purpose of determination of the rare earth elements (REE) content, and the identification of the distribution patterns of trace elements. The elemental and phase analysis experiments were conducted using the X-ray diffraction (XRD), inductively-coupled plasma spectroscopy (ICP-MS), wet chemical analysis, and field emission scanning electron microscopy equipped with energy dispersive X-ray spectroscopy (FE-SEM/EDS) techniques. The XRD results showed that the phases in the Tabas coal ash were quartz, clay minerals, alkali feldspar, magnetite, and pyrite in order of abundance. The elemental analysis showed that the major elements were Si, Al, K, Fe, Mg, S, and Na, which was in good accordance with the chemical composition of the recognized minerals by the XRD method. The concentration of REEs was varied from 0.10 ppm (for Tm) to 68.48 ppm (for Ce), with an arithmetic mean of 14.19 ppm. The abundance of 16 REE elements was or even below the average of the earth crust abundances. Only one rare earth element (Samarium) was about 4.4 and 2.2 times more abundant than in the earth crust and in the world coking coal ashes. In order to further assess the occurrence states of REEs in each of detected mineral, the Fe-SEM/EDX method was used. The SEM/EDS analysis showed that REEs were mainly concentrated in the clay minerals.

1. Introduction

The rare earth elements (REE) are classified as a group of 17 chemically similar elements including scandium, yttrium plus 15 metallic elements from the lanthanide series of the periodic table. The REEs are sub-grouped into two categories of light (LREE) and heavy rare earth elements (HREE). The light REEs are lanthanum (La), cerium (Ce), praseodymium (Pr), neodymium (Nd), promethium (Pm), samarium (Sm), europium (Eu), and gadolinium (Gd). The heavy ones are scandium (Sc), yttrium (Y), terbium (Tb), dysprosium (Dy), holmium (Ho), erbium (Er), thulium (Tm), ytterbium (Yb), and lutetium (Lu) [1]. In the recent years, REEs are extremely of great and critical importance in the various modern technology products, and consequently, play an important and vital role in the national and regional economies [1, 2]. A wide range of industry applications is listed for the REEs such as their application in the renewable energy production, televisions, generators of the wind turbines, smart cell phones, LED light bulbs, batteries, camera lenses, hard disc drives, microwaves, catalysts, medical equipments, high performance magnets, weaponry, speakers, and microphones. The surge in the global demand of REEs has been driving up the concerns about the REE supply, and this leads to an increase in

Corresponding author: gjkohan@ut.ac.ir (G. Jozanikohan).

finding the alternative REE potential resources including the coal and coal ash [3].

It is well-proved that coal is a good source for the REEs and some other trace elements [4]. Since the coal deposits are normally large enough and they have been already mined, the recovery of REEs from the coal mines is economically reasonable [1, 2]. The coal is made up of the organic and inorganic components, and it is well-known that the vast majority of the REEs in the coal are more associated with the inorganic compounds [2]. Thus if coal combusts to produce the ash, the REEs are strongly remained and enriched in the ash, and that is why the ash has been considered as a potential secondary resource for the recovery of REEs [5]. The global total concentration of REEs in the coal has been reported to be 46.3 µg/g [6], while it can reach to 62.1µg/g [7] and 120 µg/g [8] in the USA and China coals, respectively. The REE contents in the coal ash have been determined to be ten times more than what it is in the coal [9]. Many researchers have worked on the level of concentration, distribution pattern, geochemistry, and origin of REEs in different coals and coal ashes worldwide [2, 4, 5, 7-16]. There are some performed research works on the characterization of REEs in the Iranian coals or coal ashes [17-21]. In a REE study conducted on the Mazino coal mine samples, the results obtained showed an average amount of 34.74 ppm for the REE contents [17]. Another study showed that the total REE range in the Abyek coalfield, North Iran, varies between 143.19 and 254.39 ppm [18]. In another research work, the total concentration of ΣREEs in the Karmozd and Kiasar coal samples has been reported to be 69 ppm and 101 ppm, respectively [19]. It has been reported that the sum of REE concentrations in the Sangrud coal mine varied between 2.1 ppm and 117.22 ppm with an average of 34.74 ppm [20]. The average of ∑REE in the Olang coal ash, north-eastern Iran, was measured to be about 383.7 ppm [21]. The ΣREE has been increased downstream of the discharging point in the Anjir Tangeh coal washing plant located in northern Iran [22]. Most of the pervious researches have confirmed the fact that the REEs have been retained in the ash after combustion of the coals [7-22]. There are several recently performed research works in the case study of this work that were mainly concentrated on different topics including the haulage system selection [23], estimation of the optimum horizontal well depth for the gas drainage [24], the modelling metallurgical responses of the coal [25], the delineation of gas content zones [26], and the evaluation of the spontaneous combustion of coal [27]. The full study of REE contents in the Parvadeh coal ash is a task that has never been accomplished yet. However, the distribution of some selected trace elements such as V, Ni, Cd, As, and Li has been previously studied in the Parvadeh coals [28].

The general purpose of this work is to determine the REE content and the distribution pattern of trace elements in the ash samples prepared from the Parvadeh IV, B2 coal seams. Thus in this research work, a suite of coal samples was first ashed, and then was analyzed using the X-ray diffraction (XRD), inductively coupled plasma spectroscopy (ICP-MS) analysis, wet chemical analysis, and scanning electron microscopy (SEM/EDS) techniques.

2. Geological setting

The most extensive Iranian coal-bearing basin is extended in an area of 30000 km^2, locating approximately 75 km from the Tabas county, south Khorasan Province (Figure 1). The area is sub-divided into some coal-bearing zones called Mazinu, Parvadeh, and Nayband. The latitude of this area, which is classified as the eastern zone of central Iran, is between 32° 59' 48" and 32° 02' 15" N, and the longitude is between 56° 46' 30" and 56° 51' 10" E [27]. In this area, the Shotori Mountain range has been located in the east and the Kamar-Mahdi Mountains are in the west, and some other mountains of the Triassic and Jurassic age are in the south of the Parvadeh region. It is believed that the Tabas coal was initially formed along with the shale, carbonates, sandstone, and siltstones in the Late Triassic. The Ghadir member of the Nayband Formation, aging Norian, upper Triassic, contains the coal seams in this area [29].

The Parvadeh coal mine is situated in the Central Iran's structural zone, distributed in an area of 1200 km^2, and considered as one of the most extensive coking coal mines in Iran, with reserves of ~3 to ~4 Gt. The Parvadeh area is located at about 80 km south of Tabas, and surrounded by the two main faults of Nayband in the east and Naini in the west (Figure 1) [26, 29, 30]. Thus Parvadeh has been separated into six regions entitled “Parvadeh 1 to 6” by some NE-SW strike-slip faults. Moreover, some anticlines/synclines with E-W trending folds are seen in the regional faulting. The Parvadeh coal is from the bituminous type, and has a low volatile

matter, high levels of ash, and moderate to high amounts of pyrite (sulphur content). The Shemshak Group, aging lower to middle Jurassic, is composed of Nayband, Ab-Haji, Parvadeh, and Baghamshah formations, according to the age from the oldest to the youngest formations. The coal reserves are located inside the Nayband formation, and it is classified into five members, namely Gelkan, Bidestan, Howze-Sheik, Howze-Khan, and Ghadir members from base to top [30]. The economic reserves of the coal are within the Ghadir member. The thickness of the Ghadir member in the Parvadeh region is one thousand m, and composed of coal, fine argillite, sandy siltstone, sandstone, and shale as well as minor amounts of limestone. It is estimated that one billion one hundred million tons of coking coal is the reserve of the Parvardeh coal mine. The coal company in the Parvadeh region is the largest Iranian coal producer with an annual production of 5.1 million tons for raw coal as well as 0.75 million tons for concentrates. Some major faults in different geological directions have bounded and divided the Parvadeh coal mine into six sub-divisions, in which the studied area, i.e. Parvadeh IV has been chosen to make further studies. The understudied area, i.e. Parvadeh IV, has been divided by some NE-SW faults from Parvadeh III and East-Parvadeh (Figure 1) [26]. The Parvadeh different coal seams are called "A-F" based on their qualities, in which the "B2" and "C1" seams are economically minable in terms of the geo-chemical properties, thickness, and depth [26-31].

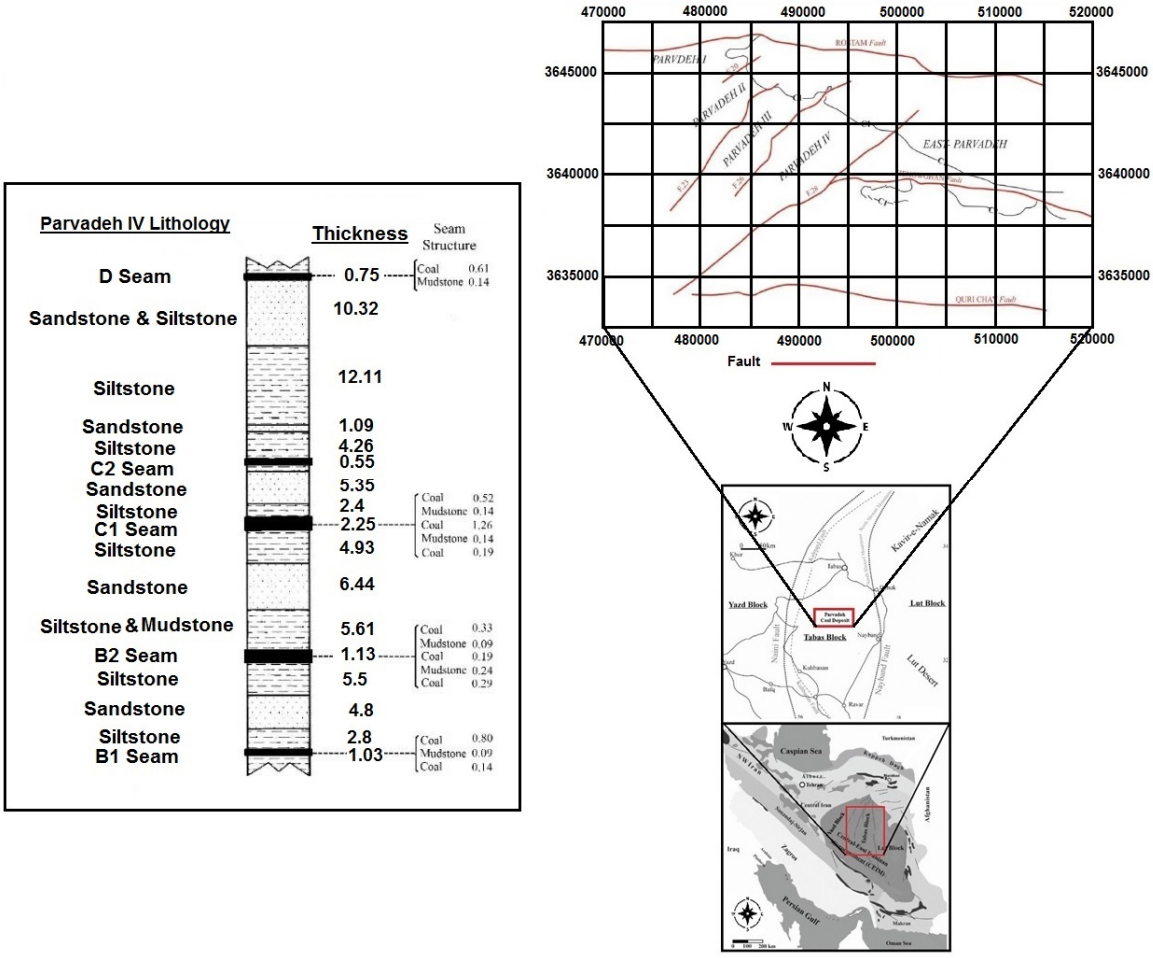

Figure 1. Location map of understudied area, modified from [26, 29].

3. Materials and methods

A suite of coal samples including 10 channel samples was collected from the Parvadeh IV coal mine. The samples were taken from the B2 seam coal (Figure 1), which was reported to have a good quality. From the lithological viewpoint, the samples were mixtures of coals and mudstone. The coal samples, as received from the field, were first reduced to a size of minus 150 mm (100 mesh). The crushed coal samples were ashed

(Figure 2) in the electrically heated thermally insulated kiln that could ash up to six samples simultaneously. The average ash content of the studied samples was 39.9315%. Then 30 g ash taken from each sample was manually ground in an agate mortar and pestle to a size of minus 75 micrometers (200 mesh), and prepared for the next several instrumental analyses.

The XRD technique has remarkably shown the ability to fully find the mineral phases in the natural samples [32]. Therefore, a D8 Advance AXS Bruker X-ray diffractometer with a 2θ/θ goniometer geometry was applied to identify the mineral phases of the ash at the X-ray laboratory, school of mining, college of engineering, University of Tehran. All the powder samples were scanned in the 2θ angular range of 4-70°. The tests were performed with the angular velocity of 1.2° per minute using copper K_α radiation (λ = 1.5406 Å) at 40 kV voltage and 30 mA. The detection limit of the quantified XRD method is about 1% [33]. The wet chemical methods including titration and gravimetric analysis were performed in order to make it clear what major elements were in the coal ash at the geochemistry laboratory, school of mining, college of engineering, University of Tehran. The detection limit of these techniques is generally 0.1 weight percent [33]. The inductively coupled plasma spectroscopy (ICP-MS) analysis was used to determine the REE content in the ash coal, with a detection limit of 1 ppm at Zarazma mineral studies laboratory, Tehran [33]. A TESCAN MIRA3 analytical field emission scanning electron microscope equipped with the energy dispersive X-ray spectroscopy (FE-SEM/EDS), SE (Secondary Electron Detector), and BSE (Back Scattered Electron Detector) helped to find the distribution of REEs in different mineral phases, and to find the mineral in which REEs were concentrated. The detection limit of the EDX analysis is ~0.1 wt.% [33]. The SEM/EDS analysis was performed at the Razi Applied Science Foundation, Tehran.

4. Results and discussion

The powder X-ray diffraction (XRD) method showed that the main mineral phases of the Tabas coal ash were quartz, clay minerals, and alkali feldspars with small amounts of magnetite and pyrite. Figure 3 shows the X-ray diffractogram of the Tabas coal ash. The main peaks of Figure 3 belong to the quartz and clay minerals. The clay minerals consisted of illite, kaolinite, and chlorite in order of abundances.

The XRD calibration curves were then prepared [34] using some different mixtures with known compositions of detected minerals in order to quantify the identified mineral phases. The observed intensities of different detected phases in the prepared mixtures (x-intercept) versus known weigh percentage of the same phase (y-intercept) were generated, and the slopes of the best fit lines were calculated for each mineral. The obtained calibration curves were then used to estimate the mineral content in the ash sample (Table 1).

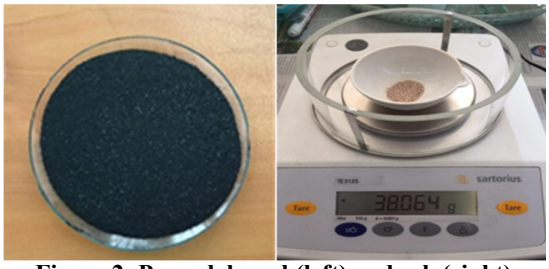

Figure 2. Parvadeh coal (left) and ash (right) samples.

Table 1. Quantified XRD results.

Mineral name	Chemical formula	Estimated weight percentage
Quartz	SiO_2	52
Clay minerals	$Al_2Si_2O_5(OH)_4$	27
Alkali feldspar	$K(AlSi_3O_8)$	13
Magnetite	Fe_3O_4	7
Pyrite	FeS_2	1

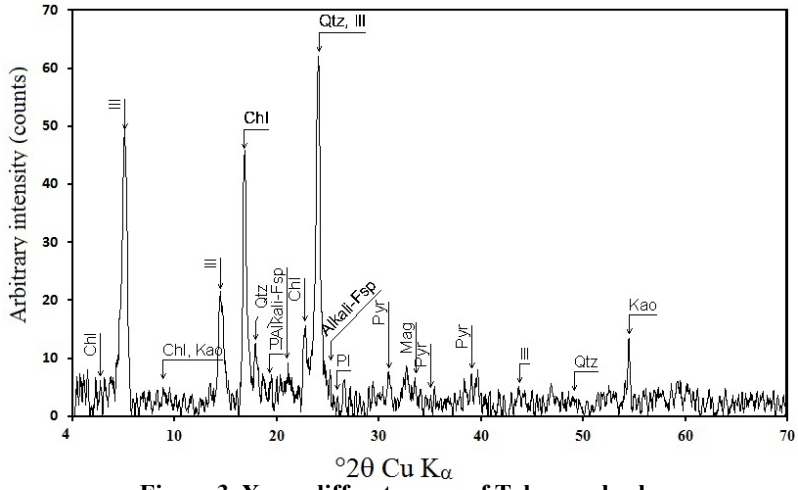

Figure 3. X-ray diffractogram of Tabas coal ash.

A series of wet chemical analysis methods including the titration and gravimetric techniques were employed to measure the Si, Al, K, Fe, Mg, Na, and S contents in every 10 ash samples. Table 2 shows the average amounts of the measured elements. As it is clear from Table 2, the main constituents of ash are aluminium and silicon. This finding was in good accordance with the mineralogical studies by the XRD method, which have already determined quartz and the clay minerals as the major phases. For every measured element by the wet chemical analyses, there was a reported mineral by the XRD method. For example, the sulphur content of the sample can be related to the pyrite, iron coming from the magnetite, pyrite, and so on.

Table 2. Average amounts of major chemical contents of Tabas coal ash.

Element symbol	Weight percentage	Element symbol	Weight percentage
Si	62.8	Al	20.3
K	9.2	Fe	5.1
Mg	1.0	S	0.98
Na	0.6		

The inductively coupled plasma spectroscopy (ICP-MS) analysis was conducted on the 10 ash samples, and showed that the concentration of REEs were more or less close to their corresponding average values in the earth crust and world coking coal ashes, except for the samarium (Table 3). Samarium was 4.4 and 2.2 times as abundant in the earth's crust and in comparison to the average amounts of it in the world coking coal ashes. In comparison to the concentrations of the rest of REEs in the earth crust and the average values of REEs in the world coking coal ashes, the REE concentration of the Parvadeh coal ash samples were not considerable. The average REE concentrations varied from 0.10 ppm (for Tm) to 68.48 ppm (for Ce), with a ΣREE of 212.78, which is higher than that in the Chinese coals (i.e. 120.6 ppm) [35]. The total summation of light REEs was higher than the same value in the heavy ones, and this is in complete accordance with the global trend of the REE distribution in the coals [36]. The value of ΣLREE/ΣHREE (3.08) showed enrichment in the light REEs (LREEs) in comparison to the heavy ones. The higher concentrations of LREEs could be due to their higher concentrations in the crust as well as the strong solubility feature of the heavy REEs (HREEs) in the complex formation. Figures 4 and 5 show the distribution pattern of the REE normalized values to upper continental crust (UCC), and chondrite normalized REE, respectively.

From Figures 4 and 5, it is clear that the slope of La-Nd is relatively constant but the slope of Sm-Er is glacis. The values of Sm and Tm showed a "V" shape and clear Tm, and an Lu discrepancy in Figures 4 and 5. The positive Sm anomalies were observed in the distribution pattern of the ash samples, showing a slightly LREE enrichment. The REE distribution patterns of all the studied samples were completely similar due to the similarities in the depositional environment. Samarium is almost ~2.2 times more abundant than in the world coking coal ashes.

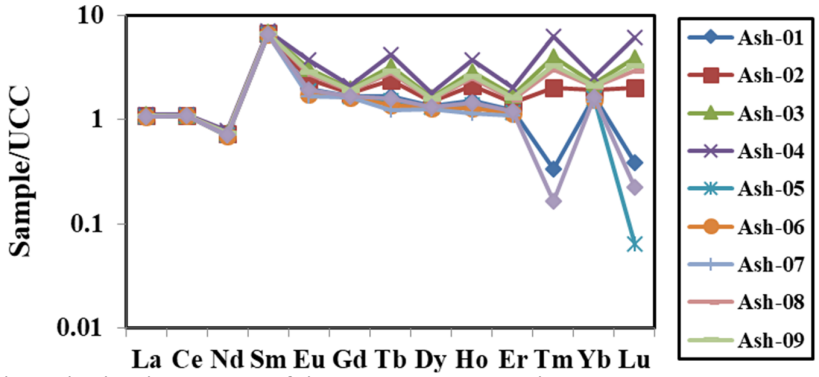

Figure 4. Normalized distribution pattern of light and heavy REEs in Tabas coal ashes to the upper continental crust.

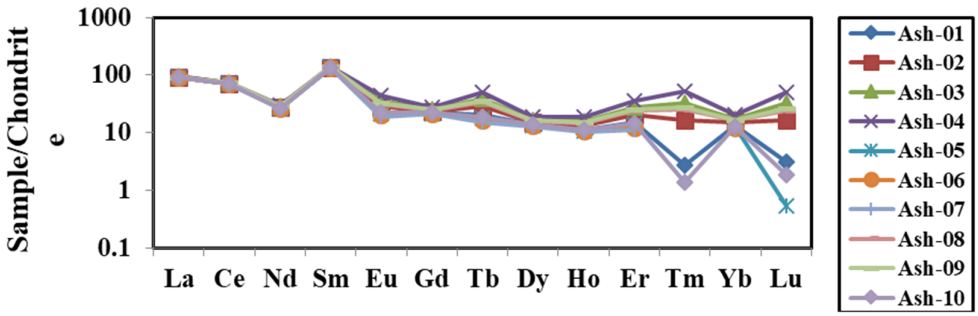

Figure 5. Normalized distribution pattern of light and heavy REEs in Tabas coal ashes to the chondrite.

Table 3. Average amounts of REEs in comparison to their average amounts in the earth crust [37], chondrite [38], and world coking coal ashes [39].

Element symbol	Atomic number	Average (ppm)	Earth curst (%) [37]	Chondrite values (%) [38]	Average in world coking coal ashes [39]
Sc	21	17.82	22.00		24.0
Y	39	20.34	33.00		57.0
La	57	33.26	39.00	0.37	76.0
Ce	58	68.48	66.50	0.96	140.0
Pr	59	N.D	9.20	0.14	26.0
Nd	60	19.22	41.50	0.71	75.0
Pm	61	N.D	---	---	N.D
Sm	62	31	7.05	0.23	14.0
Eu	63	1.96	2.00	0.09	2.6
Gd	64	6.75	6.20	0.31	16.0
Tb	65	1.16	1.20	0.06	2.1
Dy	66	5.25	5.20	0.38	15.0
Ho	67	1.26	1.30	0.09	4.8
Er	68	2.82	3.50	0.25	6.4
Tm	69	0.10	0.52	0.04	2.2
Yb	70	3.24	3.20	0.25	6.9
Lu	71	0.12	0.80	0.04	1.3
ΣREE		212.78	242.17		469.3
ΣLREE		160.67	171.45		349.6
ΣHREE		52.11	70.72		119.7
ΣLREE/ΣHREE		3.08	2.42		2.92

A representative ash sample was chosen to be further assessed by the scanning electron microscopy (SEM/EDS) technique. The sample was coated with a thin layer of gold for several times. The golden coating promotes the sample conductivity, prevents from the surface charging, and provides a homogeneous surface, which is better for the imaging and further analysis [40, 41]. The method was used to study the distribution of elements, especially REEs on the each mineral. Figures 6-9 show the SEM micrographs of Tabas coal ash.

The EDX elemental mapping showed that the platy particles were mostly aluminosilicates, i.e. the clay minerals (Table 4, and Fig. 10). From the SEM images, it is clear that the most dominant phase in the studied samples was clay minerals with platy morphology. Kaolinite was mainly observed in the form of thin idiomorphic platelets (e.g. Figures 7 and 8), and filled most of the pore spaces along with chlorite. Illite was found as lath shape (Figure 6). The results obtained show an enrichment of REEs, especially Samarium in the platy particles, i.e. clay minerals. Thus it seems that REEs were mostly concentrated in the clay minerals. The particle size measurements showed a big variation in the clay mineral sizes. The smallest and largest plates were 0.10 and 20 micrometers, respectively. The average size of the plates was 0.74 micrometers.

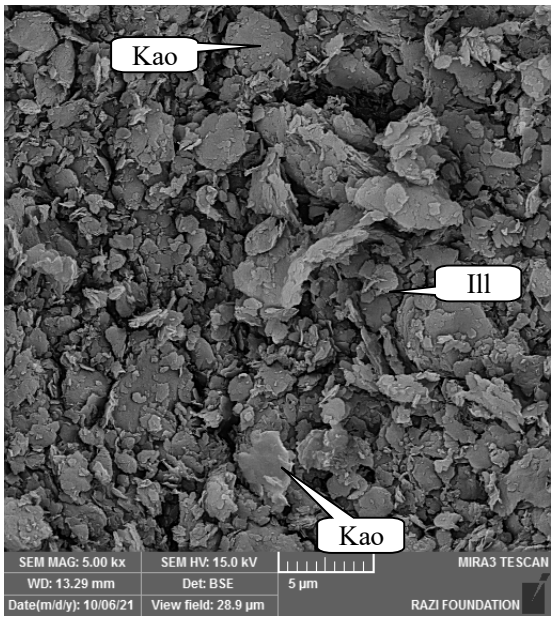

Figure 6. General view of Tabas coal ash under SEM, magnitude 5000, WD: 13.29 mm. Kao: kaolinite, Ill: Illite.

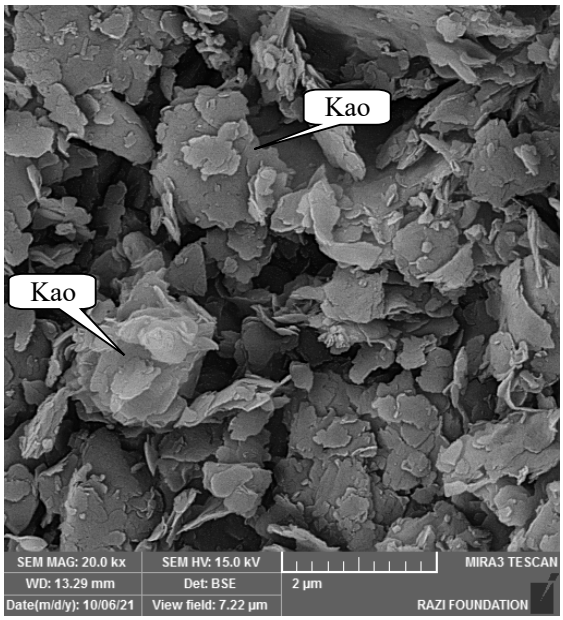

Figure 7. SEM images of clay minerals general view of Tabas coal ash, magnitude 20000, WD: 13.29 mm. Kao: kaolinite.

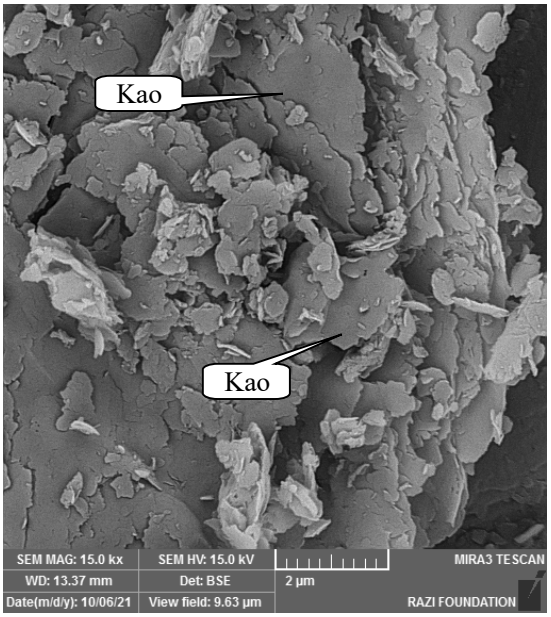

Figure 8. Size variation in the platy fabric of Tabas coal ash, magnitude 15000, WD: 13.37 mm. Kao: kaolinite.

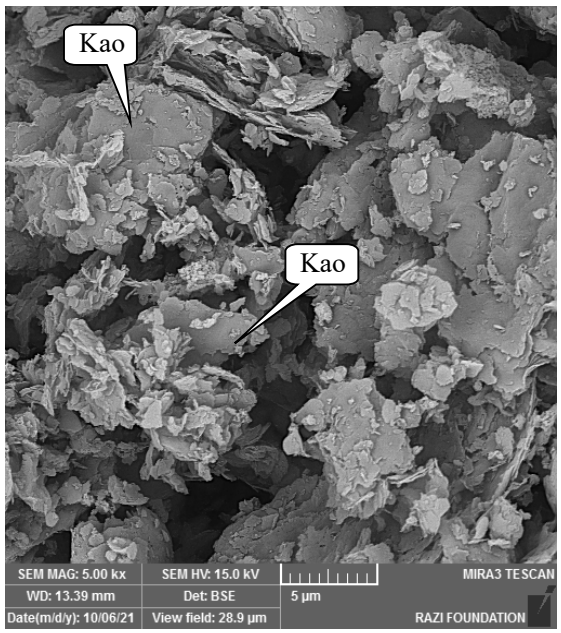

Figure 9. Platy morphology of the clay minerals in Tabas coal ash, magnitude 5000, WD: 13.39 mm. Kao: kaolinite.

Table 4. Elemental distribution in Tabas coal ash, provided by X-ray mincroanalysis (EDS)

Elt	Line	Int	Error	K	Kr	W%	A%	ZAF	Formula	Ox%	Pk/Bg	Class	LConf	HConf	Cat#
C	Ka	54.1	60.9650	0.2668	0.1185	35.95	53.58	0.3296		0.00	288.80	A	34.70	37.20	0.00
O	Ka	88.4	62.9804	0.2137	0.0949	31.05	34.75	0.3056		0.00	198.73	A	30.21	31.90	0.00
Al	Ka	105.6	68.0188	0.0840	0.0373	5.31	3.52	0.7026		0.00	112.01	A	5.18	5.44	0.00
Si	Ka	148.2	69.0265	0.1233	0.0547	7.44	4.74	0.7359		0.00	157.41	A	7.28	7.59	0.00
K	Ka	24.4	3.2050	0.0353	0.0157	1.81	0.83	0.8654		0.00	15.52	A	1.72	1.90	0.00
Ca	Ka	7.1	3.2486	0.0115	0.0051	0.57	0.25	0.8974		0.00	6.15	A	0.51	0.62	0.00
Sc	Ka	4.7	3.2922	0.0084	0.0037	0.44	0.17	0.8483		0.00	4.49	A	0.39	0.49	0.00
Y	La	14.9	94.2186	0.0233	0.0104	1.57	0.32	0.6611		0.00	16.72	A	1.46	1.67	0.00
La	La	5.7	4.8620	0.0305	0.0135	1.96	0.25	0.6906		0.00	3.56	B	1.75	2.17	0.00
Ce	La	4.9	4.9056	0.0283	0.0126	1.82	0.23	0.6932		0.00	3.33	B	1.61	2.03	0.00
Pr	La	2.2	4.9492	0.0137	0.0061	0.87	0.11	0.6975		0.00	3.15	B	0.72	1.02	0.00
Pm	La	1.4	5.0365	0.0101	0.0045	0.66	0.08	0.6835		0.00	3.04	B	0.51	0.80	0.00
Sm	La	2.7	5.0801	0.0215	0.0095	1.42	0.17	0.6738		0.00	3.01	B	1.20	1.63	0.00
Eu	La	2.3	5.1237	0.0193	0.0086	1.28	0.15	0.6710		0.00	2.81	B	1.06	1.50	0.00
Ho	La	1.8	5.2981	0.0223	0.0099	1.56	0.17	0.6333		0.00	2.40	B	1.26	1.86	0.00
Er	La	1.1	5.3417	0.0158	0.0070	1.11	0.12	0.6277		0.00	2.46	B	0.84	1.39	0.00
Tm	La	2.6	5.3853	0.0406	0.0180	2.88	0.31	0.6252		0.00	2.41	B	2.42	3.34	0.00
Lu	La	1.6	5.4725	0.0316	0.0141	2.31	0.24	0.6093		0.00	2.28	B	1.83	2.78	0.00
				1.0000	0.4440	100.00	100.00			0.00					0.00

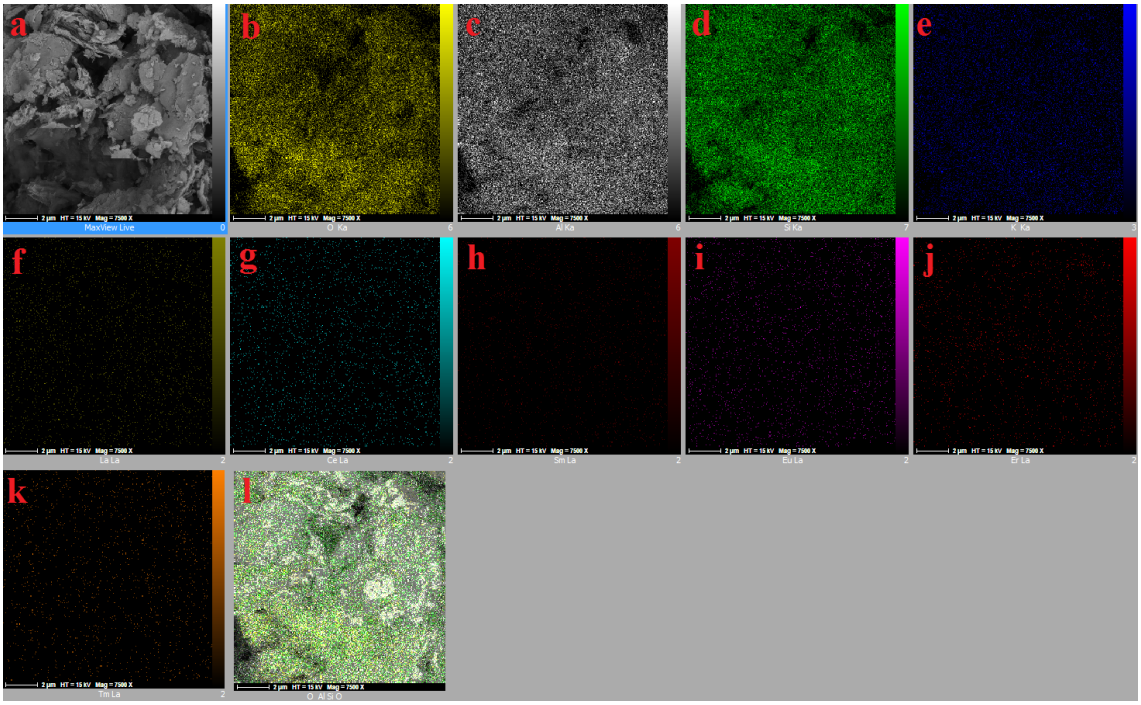

Figure 10. Elemental mapping of Tabas coal ash, provided by the he field emission scanning electron microscope (FE-SEM) including: (a) the whole SEM image, (b) oxygen (O_2), (c) aluminium (Al), (d) silicon (Si), (e) potassium (K), (f) lanthanum (La), (g) cerium (Ce), (h) samarium (Sm), (i) europium (Eu), (j) erbium (Er), (k) thulium (Tm), (l) oxygen, aluminium, and silicon (O_2, Al, Si).

5. Conclusions

In this research work, XRD, inductively coupled plasma spectroscopy (ICP-MS) analysis, wet chemical analysis, and field emission scanning electron microscopy equipped with energy dispersive X-ray spectroscopy (FE-SEM/EDS) were employed to determine the REE distribution in the Tabas coal ash. Several mineral phases including quartz, clay minerals, alkali feldspars, magnetite, and pyrite were identified in the Tabas coal ash. Among the detected phases in the coal, the clay minerals seemed to be the host of REEs. The concentration of REEs varied from 0.10 ppm (for Tm) to 68.48 ppm (for Ce), with an arithmetic mean of 14.19 ppm. The concentration of REEs was more or less close to their corresponding average values in the earth crust, except for the samarium, which was 4.4 and 2.2 times more abundant in the earth's crust and its average amount in the world coking coal ashes. The total summation of the light REEs was higher than the same value in the heavy ones, and this is in

complete accordance with the global trend of REE distribution in the coals.

Acknowledgement

The authors would like to acknowledge the X-ray laboratory, School of Mining, College of Engineering, University of Tehran for kind participation and collaborations made throughout the present work.

References

[1]. Balaram, V. (2019). Rare earth elements: A review of applications, occurrence, exploration, analysis, recycling, and environmental impact. Geoscience Frontiers. 10 (4): 1285-1303.

[2]. Lin, R., Howard, B.H., Roth, E.A., Bank, T.L., Granite, E.J. and Soong, Y. (2017). Enrichment of rare earth elements from coal and coal by-products by physical separations. Fuel, 200, 506-520.

[3]. Jowitt, S. M., Werner, T.T., Weng, Z., and Mudd, G.M. (2018). Recycling of the rare earth elements. Current Opinion in Green and Sustainable Chemistry, 13, 1-7.

[4]. Seredin, V.V., Dai, S., Sun, Y. and Chekryzhov, I.Y. (2013). Coal deposits as promising sources of rare metals for alternative power and energy-efficient technologies. Applied Geochemistry, 31, 1-11.

[5]. Dai, S., Ward, C.R., French, D. and Hower, J.C. (2018). Comments on geochemical characteristics of rare metal, rare-scattered, and rare earth elements and minerals in the late permian coals from the Moxinpo mine, Chongqing, china. Energy and Fuels. 32 (8): 8891-8894.

[6]. Valkovic, V., Trace Elements in coal, Boca Raton: CRC Press, 1983, Vol. 1, 210 pp. Vol. 2, 281 pp.

[7]. Finkelman, R.B. (1993). Trace and minor elements in coal. In Organic geo-chemistry (pp. 593-607). Springer, Boston, MA.

[8]. Dai, S., Zhou, Y., Ren, D., Wang, X., Li, D. and Zhao, L. (2007). Geo-chemistry and mineralogy of the Late Permian coals from the Songzo Coalfield, Chongqing, southwestern China. Science in China Series D: Earth Sciences, 50(5), 678-688.

[9]. Seredin, V.V. and Finkelman, R.B. (2008). Metalliferous coals: a review of the main genetic and geochemical types. International Journal of Coal Geology. 76 (4): 253-289.

[10]. Zou, J., Tian, H. and Wang, Z. (2017). Leaching process of rare earth elements, gallium, and niobium in a coal-bearing strata-hosted rare metal deposit—A case study from the Late Permian tuff in the Zhongliangshan mine, Chongqing. Metals. 7 (5): 174.

[11]. Dai, S., Finkelman, R.B., French, D., Hower, J.C., Graham, I.T. and Zhao, F. (2021). Modes of occurrence of elements in coal: A critical evaluation. Earth-Science Reviews, 103815.

[12]. Montross, S.N., Verba, C.A., Chan, H.L. and Lopano, C. (2018). Advanced characterization of rare earth element minerals in coal utilization by-products using multimodal image analysis. International Journal of Coal Geology, 195, 362-372.

[13]. Zhao, S., Duan, Y., Lu, J., Gupta, R., Pudasainee, D., Liu, S. and Lu, J. (2018). Chemical speciation and leaching characteristics of hazardous trace elements in coal and fly ash from coal-fired power plants. Fuel, 232, 463-469.

[14]. Chen, G., Sun, Y. Wang, Q., Yan, B., Cheng, Z. and Ma, W. (2019). Partitioning of trace elements in coal combustion products: A comparative study of different applications in China. Fuel, 240, 31-39.

[15]. Franus, W., Wiatros-Motyka, M. M., and Wdowin, M. (2015). Coal fly ash as a resource for rare earth elements. Environmental Science and Pollution Research. 22 (12): 9464-9474.

[16]. Kursun Unver, I. and Terzi, M. (2018). Distribution of trace elements in coal and coal fly ash and their recovery with mineral processing practices: A review. Journal of Mining and Environment. 9 (3): 641-655.

[17]. Pazand, K. (2015). Rare earth element geochemistry of coals from the Mazino Coal Mine, Tabas Coalfield, Iran. Arabian Journal of Geosciences. 8 (12): 10859-10869.

[18]. Pazand, K. (2015). Geo-chemical properties of rare earth elements (REEs) in coals of Abyek coalfield, North Iran. Arabian Journal of Geosciences. 8 (7): 4855-4862.

[19]. Moore, F. and Esmaeili, A. (2012). Mineralogy and geochemistry of the coals from the Karmozd and Kiasar coal mines, Mazandaran province, Iran. International journal of coal geology. 96: 9-21.

[20]. Pazand, K. (2015). Characterization of REE geo-chemistry of coals from the Sangrud coal mine, Alborz coalfield, Iran. Arabian Journal of Geosciences. 8 (10): 8277-8282.

[21]. Taghipour, N. and Solaymani, M.Z. (2015). Geo-chemistry and origin of elements of Upper Triassic Olang coal deposits in north-eastern Iran.

[22]. Shahhosseini, M., Ardejani, F.D. and Baafi, E. (2017). Geo-chemistry of rare earth elements in a neutral mine drainage environment, Anjir Tangeh, northern Iran. International Journal of Coal Geology. 183: 120-135.

[23]. Ghasvareh, M. A., Safari, M. and Nikkhah, M. (2019). Haulage system selection for Parvadeh Coal

Mine using multi-criteria decision-making methods. Mining Science: 26.

[24]. Taheri, A. and Sereshki, F. (2017). Estimate of the optimum horizontal well depth for gas drainage using a numerical method in the Tabas coal mine. Research Online: Coal Operators' Conference, University of Wollongong.

[25]. Alidokht, M., Yazdani, S., Hadavandi, E. and Chelgani, S.C. (2021). Modeling metallurgical responses of coal Tri-Flo separators by a novel BNN: A "Conscious-Lab" development. International Journal of Coal Science and Technology, 1-11.

[26]. Molayemat, H. and Mohammad Torab, F. (2017). Evaluation of coalbed methane potential in Parvadeh IV coal deposit in central Iran using a combination of MARS modeling and Kriging. Journal of Mining and Environment. 8 (2): 305-319.

[27]. Saffari, A., Ataei, M. and Sereshki, F. (2019). Evaluation of the spontaneous combustion of coal (SCC) using the R70 test method based on the correlation among intrinsic coal properties (Case study: Tabas Parvadeh coal mines, Iran). Rudarsko-geološko-naftni zbornik. 34 (3).

[28]. Rajabzadeh, M.A. Ghorbani, Z. and Keshavarzi, B. (2016). Chemistry, mineralogy, and distribution of selected trace elements in the Parvadeh coals, Tabas, Iran. Fuel, 174, 216-224.

[29]. Salehi, M.A., Moussavi-Harami, R., Mahboubi, A. and Rahimi, B. (2014). Palaeoenvironment and basin architecture of the Lower Jurassic Ab-Haji Formation, east-central Iran.

[30]. Nia, H.S. (1994). Geological characteristics of the Parvadeh region of the Tabas coal-bearing basin, Central Iran. The AAPG/Datapages Combined Publications Database, CSPG Special Publications.

[31]. Hashemi, S.M. (2010). Minerals of coal main seam in Parvade coalfield (Tabas–Iran). In The 1st International Applied Geological Congress, Department of Geology, Islamic Azad University–Mashad Branch, Iran (pp. 26-28).

[32]. Jozanikohan, G., Sahabi, F., Norouzi, G.H., Memarian, H. and Moshiri, B. (2016). Quantitative analysis of the clay minerals in the Shurijeh Reservoir Formation using combined X-ray analytical techniques. Russian Geology and Geophysics. 57 (7): 1048-1063.

[33]. Patnaik, P. (2004). Dean's analytical chemistry handbook. McGraw-Hill Education.

[34]. Jozanikohan, G. (2017). On the development of a non-linear calibration relationship for the purpose of clay content estimation from the natural gamma ray log. International Journal of Geo-Engineering. 8 (1): 1-18.

[35]. Dai, S., Li, D., Chou, C.L., Zhao, L., Zhang, Y., Ren, D. and Sun, Y. (2008). Mineralogy and geochemistry of boehmite-rich coals: new insights from the Haerwusu Surface Mine, Jungar Coalfield, Inner Mongolia, China. International Journal of Coal Geology. 74 (3-4): 185-202.

[36].Dai, S., Ren, D., Hou, X. and Shao, L. (2003). Geo-chemical and mineralogical anomalies of the late Permian coal in the Zhijin coalfield of southwest China and their volcanic origin. International Journal of Coal Geology. 55 (2-4): 117-138.

[37]. Lide, D.R. (Ed.) (2004). CRC handbook of chemistry and physics (Vol. 85). CRC press.

[38]. Potin, S., Beck, P., Bonal, L., Schmitt, B., Garenne, A., Moynier, F. and Quirico, E. (2020). Mineralogy, chemistry, and composition of organic compounds in the fresh carbonaceous chondrite Mukundpura: CM1 or CM2? Meteoritics and Planetary Science. 55 (7): 1681-1696.

[39]. Wang, Z., Dai, S., Zou, J., French, D. and Graham, I.T. (2019). Rare earth elements and yttrium in coal ash from the Luzhou power plant in Sichuan, Southwest China: Concentration, characterization and optimized extraction. International Journal of Coal Geology, 203, 1-14.

[40]. Leslie, S.A. and Mitchell, J.C. (2007). Removing gold coating from SEM samples. Palaeontology. 50 (6): 1459-1461.

[41]. Kim, K.H., Akase, Z., Suzuki, T. and Shindo, D. (2010). Charging effects on SEM/SIM contrast of metal/insulator system in various metallic coating conditions. Materials transactions, 1005171076-1005171076.

مطالعه ژئوشیمیایی محتوای عناصر نادر خاکی در خاکستر زغال طبس، معدن زغال پروده

گلناز جوزانی کهن*[۱]، محسن نصرتی ابرقوئی[۲] و حسن صدیقی[۳]

۱- دانشکده مهندسی معدن، دانشکده فنی، دانشگاه تهران، تهران، ایران
۲- دانشکده معدن و متالورژی، دانشگاه یزد، یزد، ایران
۳- مجری و سرپرست طرح عناصر نادر خاکی، سازمان توسعه و نوسازی معادن و صنایع معدنی ایران (ایمیدرو)، تهران، ایران

ارسال ۲۰۲۱/۱۰/۲۱، پذیرش ۲۰۲۲/۱/۱۳

* نویسنده مسئول مکاتبات: gjkohan@ut.ac.ir

چکیده:

وسیع‌ترین حوزه زغال‌دار ایران با وسعت ۳۰،۰۰۰ کیلومتر مربع در ۷۵ کیلومتری شهرستان طبس در استان خراسان جنوبی قرار دارد. در این مقاله، خاکستر زغال‌سنگ طبس به منظور تعیین محتوای عناصر کمیاب خاکی (REE) و شناسایی الگوهای توزیع عناصر کمیاب مورد مطالعه و بررسی قرار گرفت. آزمایش‌های آنالیز عنصری و فازی با استفاده از پراش پرتو ایکس (XRD)، طیف‌سنجی پلاسمای جفت شده القایی (ICP-MS)، تجزیه و تحلیل شیمی تر، میکروسکوپ الکترونی روبشی نشر میدانی مجهز به طیف‌سنج پرتوی ایکس نوع ED (FE-SEM/EDS) انجام شد. نتایج پراش پرتو ایکس (XRD) نشان داد که فازهای خاکستر زغال‌سنگ طبس به ترتیب فراوانی، کوارتز، کانی‌های رسی، فلدسپات قلیایی، مگنتیت و پیریت است. عناصر اصلی براساس نتایج تجزیه عنصری شامل Si، Al، K، Fe، Mg، S و Na است که منطبق با ترکیب شیمیایی کانی‌های شناسایی شده به روش XRD هست. براساس آنالیزهای انجام شده مقدار عناصر خاکی کمیاب از ۰،۱۰ ppm (برای Tm) تا ۶۸،۴۸ ppm (برای Ce) با میانگین حسابی ۱۴،۱۹ ppm متغیر بوده و فراوانی ۱۶ عنصر REE کمتر از میانگین فراوانی پوسته زمین است و تنها عیار یک عنصر خاکی کمیاب (ساماریوم) در حدود ۴،۴ و ۲،۲ برابر بیشتر از پوسته زمین و خاکستر زغال سنگ‌های کک‌شونده جهان بود. برای ارزیابی بیشتر فازهای تمرکزدهنده عناصر REE در هر کانی شناسایی شده، از روش Fe-SEM/EDX استفاده شد. تجزیه و تحلیل SEM/EDS نشان داد که عناصر خاکی کمیاب عمدتاً در کانی‌های رسی متمرکز شده‌اند.

کلمات کلیدی: آنالیز عناصر کمیاب خاکی (REE)، روش پراش پرتو ایکس (XRD)، روش طیف‌سنجی پلاسمای جفت‌شده القایی (ICP-MS)، توزیع عناصر کمیاب خاکی، ژئوشیمی عناصر کمیاب خاکی